Digital Magnetic Compass With Smart Correction Function - Recent Experimental Results and Further Works -

Jeong-Bin YIM*, Yeong-Ho SHIM**, Chang-Kyeong KIM**, Gi-Young CHOI**
*Mokpo Maritime University (MMU), 571-2, Jukyo-dong, Mokpo, Junnam, 530-729, Korea, jbyim@mmu.ac.kr
**Graduate School of MMU, 571-2, Jukyo-dong, Mokpo, Junnam, 530-729, Korea

Key words: digital magnetic compass, smart correction, fluxgate sensor, polynomial regression, phase sensitive detector

ABSTRACT

The paper describes recent experimental results on the development of Digital Magnetic Compass (DMC), which can provide smart automatic correction functions to the magnetic interferences. The design methodology of magnetic sensing circuit with ring-core fluxgate sensor is represented. The performance results of the sensing circuits are discussed with error analysis by polynomial regressions. As test results, the sensing circuit filtered only the second harmonic signal that is proportional to the direction of earth's magnetic field, and it leads to the obtainment of bearing information. In addition, the total residual errors of DMC can be analyzed by the adoption of polynomial regressions. It shown that the possibility of high precise DMC, in the future.

1. Introduction

Recently, Fluxgate sensors are used to measure the target bearing in many practical fields. Traditionally, the magnetic compass has been used in navigation for centuries. Advances in technology have led to the solid-state electronic compass based on Fluxgate magnetic sensors. Electronic compasses offer many advantages over conventional needle type or gimbaled compasses such as: shock and vibration resistance, electronic compensation for stray field effects, and direct interface to electronic navigation systems. Fluxgate has been and is the workhorse of magnetic field strength instruments both on earth and in space. It is rugged, reliable, and physically small and requires very little power to operate. These characteristics, along with its ability to measure the vector components of magnetic fields over a 0.1 nT to 1 mT range from DC to several kHz, make it a very versatile instrument. This sensor provides a low cost means of magnetic field detection. Geologists use them for exploration, geophysicists use them to study the geomagnetic field, scientists use them in their research, and the military use them in many applications including mine detection, vehicle detection, and target recognition (Dept. US Navy, 1994; Lauro O. *etc*, 2000; Erick B.P., *etc*, 1999). We use them for the Digital Magnetic Compass (DMC) to measure the target bearing with automatic interferences corrections.

The development of highly precise DMC, which can provide smart correction functions of magnetic interferences, is the last target of this study. To attain the last target, this research will extend to several works such as; the optimal designs of Fluxgate sensor with high resolution, the circuit designs of high Q-factored Phase Sensitive Detector (PSD) using analog close-loop circuit, and the design of digital filters providing automatic real-time correction of external magnetic interferences using built-in digital signal processor. In this work, some recent experimental results on the circuit implementations and experimental results are represented. Further works to achieve the last goal of DMC are also discussed.

2. Basic of Magnetic Sensing

2.1 Earth's Magnetic Field

The earth's magnetic field intensity is approximately 30,000 nT at the equator and 60,000 nT at the poles on the surface and has a component parallel to the earth's surface that always point toward magnetic north. This is the basis for all magnetic compasses. The key words here are parallel to the earth's surface and magnetic north.

Figure 1 shows how the earth's magnetic field (F_T) is composed of a horizontal (F_H) and a vertical (F_V) component. The angle between the magnetic field and the horizontal component is known as Inclination (Ψ_I). It is well known that the earth's magnetic poles do not correspond with its geographic poles. Furthermore, the magnetic field is not perfectly uniform it is irregular. This phenomenon is called Variation (Ψ_V) that is the angle between true north and the horizontal trace of the magnetic field (YIM J.B., 1995).

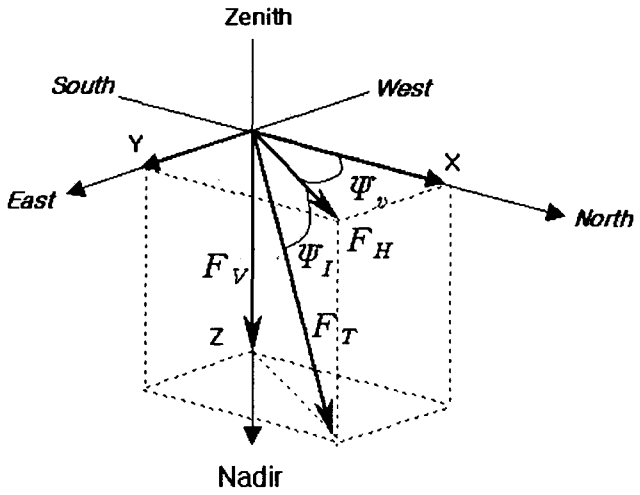

Figure 1 Vector magnetic components: Variation (Ψ_v), Inclination (Ψ_I), Horizontal Intensity (F_H), Vertical Intensity (F_V), and Total Intensity (F_T).

A good compass should point in the directions of the horizontal component of the magnetic field where the compass is located. The key to accurately finding a compass heading, or azimuth, is to determine the Horizontal intensity (F_H) of the earth's magnetic field.

2.2 Measuring Magnetic Field

Today, there are several types of electronic compasses to chose from: Fluxgate, Magneto-resistive, Magneto-inductive, and others. One way to classify the various magnetic sensors is by the field sensing range. Table 1 lists the various sensor technologies and illustrates the magnetic field sensing ranges. A common type of magnetic sensor for navigation systems is the Fluxgate sensor as shown in Table 1 (Michael J.C., *etc*).

Table 1 Magnetic sensor technology and field ranges.

Magnetic Sensor Technology	Detectable Filed Range (Gauss)									
	10^{-8}		10^{-4}		10^{0}		10^{4}		10^{8}	
Squid										
Fiber-Optic										
Optically Pumped										
Muclear Procession										
Search-Coil										
Flux-Gate										
Magnetotransistor										
Magnetodiode										
Magneto Optical Sensor										
Giant Magnetoresistive										
Hall-Efect Sensor										
Earth's Field										

Figure 2 illustrates the configurations of two-channel ring-core Fluxgate sensor with magnetic toroidal core and the associated windings that senses the surrounding magnetic field. A drive winding is wound around a toroidal core, high-permeability magnetic core. The two sense windings are wound around the toroidal core at right angles to one another to sense orthogonal components of a surrounding magnetic field (Kristin L.M., 2001; US Patent, 1981; US Patent, 1987; NEXEN Co. Korea).

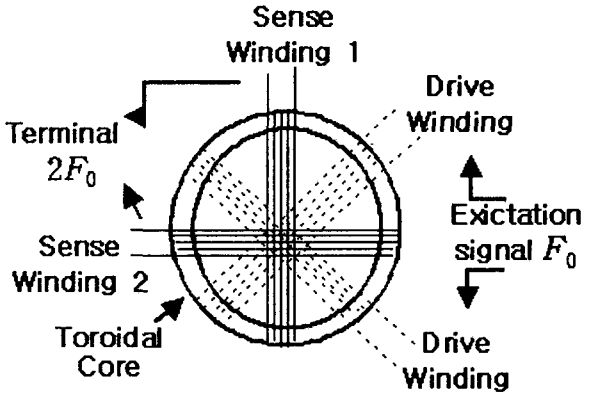

Figure 2 Configurations of two-channel ring-core Fluxgate sensor with toroidal excitation.

Figure 3 shows fictitious waveforms to explain the electrical operation of the two-channel ring-core Fluxgate sensor. The waveform A is a excitation voltage applied to the drive winding with frequency (F_0), and the waveform B represents induced magnetization in the sense winding 1 and sense winding 2. In the absence of external magnetic filed, the two sense windings are saturated at a same time each other as shown in the waveform C. Thus, the net output from the terminal is to be zero. While, in the presence of an external magnetic filed, one sense winding saturates before the other sense winding saturates. The output waveforms from each of the two sense windings make the time difference (τ) as shown in the waveform D. The time difference (τ) is proportional to the phase difference ($\Delta\Phi$) between the sense winding 1 and sense winding 2. Thus, the net output from the terminal is a pulse-like whose length and peak voltages is a function in the external magnetic field as shown in the waveform E. The frequency of the output signal from the terminal is twice ($2F_0$) the excitation frequency (F_0) since the saturation-to-saturation transition occurs twice each excitation period.

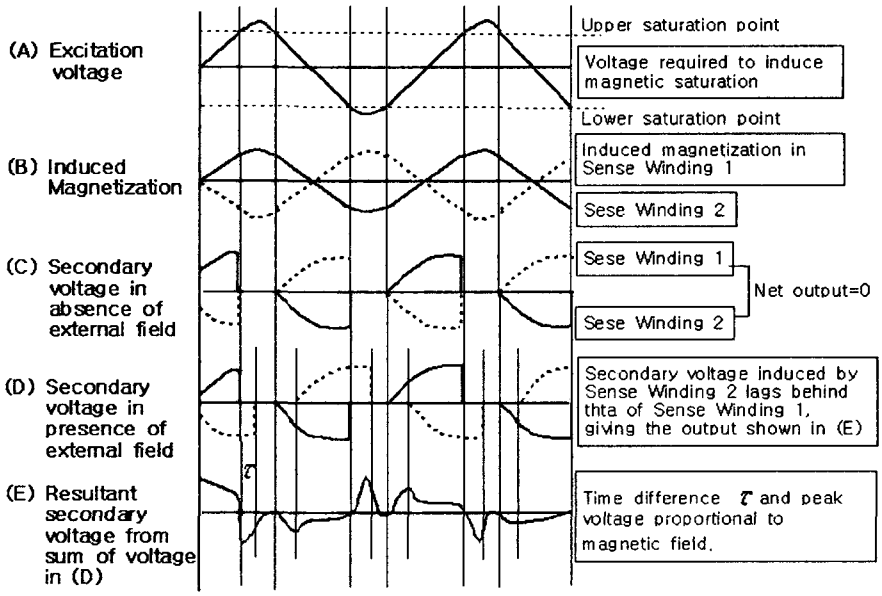

Figure 3 Fictitious waveforms for the electrical operation of the two-channel ring-core Fluxgate sensor.

3. Circuit Design

3.1 Configuration of DMC

The circuit configurations of Digital Magnetic Compass (DMC) with Fluxgate sensor are shown in Figure 4. It consists of Excitation Circuit, Fluxgate Sensor, Phase Sensitive Detector (PSD), and Smart Digital Correction

System. In this paper, some implementation results on the circuit design of DMC are represented except for the parts of Digital Signal Processing and Display in the Smart Digital Correction system.

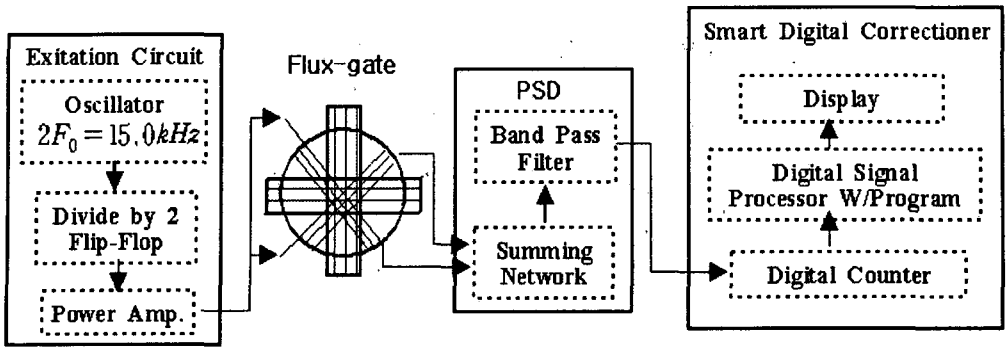

Figure 4 Circuit configurations of DMC.

3.2 Circuit Design

Excitation Circuit

Excitation Circuit consists of the oscillator tuned to twice the excitation frequency (F_0 =7.5kHz), the flip-flop (F/F) which divides the oscillator frequency by two and the power amplifier which is driven by the F/F and, in turn, provides the excitation current to the excitation winding. Here, The drive windings are driven at 7.5kHz square shaped bi-directional current pulse train, optimized to minimize the Fluxgate noise.

PSD

In the presence of an external magnetic field, a second harmonic of the excitation signal is generated in the sense winding. The phase of sense winding signal with respect to the drive winding represents the direction of the magnetic field component. The signal from the sense winding is then fed to the Phase Sensitive Detector (PSD). The output of PSD is a maximum when the input signal is at the same frequency and in phase with a reference signal. It detects the phase difference ($\Delta\Phi$), which is extracted from summing network. In mechanical terms, PSD works by switching the input signal on and off at the reference frequency (F_r). If the input signals are in phase (*i.e.*, $2F_0 = F_r$), the output is a rectified version of the input signal. If they are not in phase (*i.e.*, $2F_0 \neq F_r$), the DC output is proportional to the cosine of the phase difference. This type of PSD is one of a high-Q band-pass filter that amplifies frequencies only near a desired frequency (in this case $2F_0$ =15.0kHz). In this work, twin-T networked band-pass active filter is designed and realized as shown in Figure 5 (Texas Instrument, 2001). The signal from the PSD is then fed to the Smart Digital Correction system.

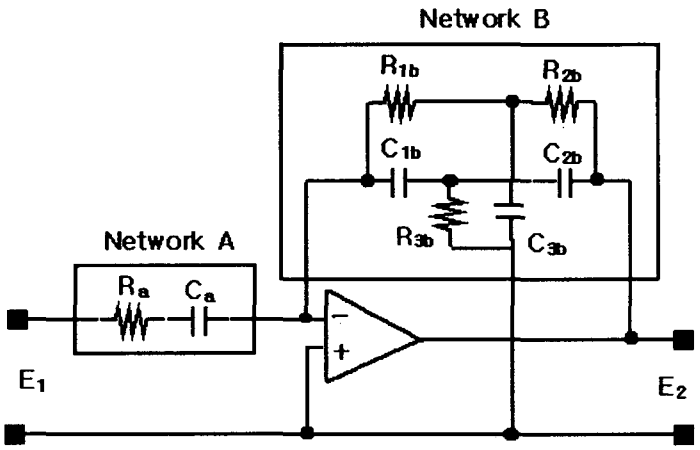

Figure 5 Circuit design of single feedback band-pass filter to implement PSD.

Smart Digital Correction System

The Smart Digital Correction system consists of Digital Counter, Digital Signal Processor with built-in program to correct external magnetic interferences automatically, and Displayer. The whole circuit design works of this system are now under proceeding.

Figure 6 shows the circuit configuration of Digital Counter with the discrimination circuit to decide turning direction of DMC. The bearing information draws from the phase differences between the output signals of PSD and the reference signals in EC. The degrees of compass bearing are proportional to the differences between $\Delta\Phi$ (the output signal of PSD) and Φ_r (the reference signal in EC).

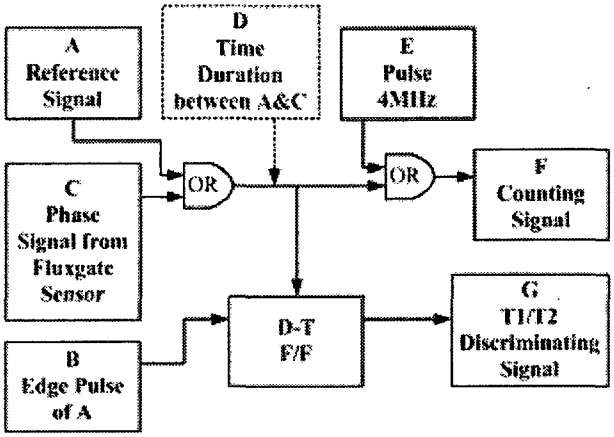

Figure 6 Circuit configuration of Digital Counter with the discrimination circuit.

The detailed circuit design, mentioned above, and implementation results for the EC, PSD, and Digital Counter are described in the previous works by the authors (YIM J. B., 2002a; YIM J. B., 2002b).

4. Experiments And Results

4.1 Experimental Environments

Figure 7 shows test environmental set-up in a normal laboratory without any electrical interference shielding. The test circuit, which is composed of Excitation Circuit, Fluxgate Sensor, and Digital Count, is located upper the plastic compass card apart by 60cm to avoid magnetic interferences of step motor. The step motor is attached to the bottom of compass card and it provides turning the compass card as required step angle.

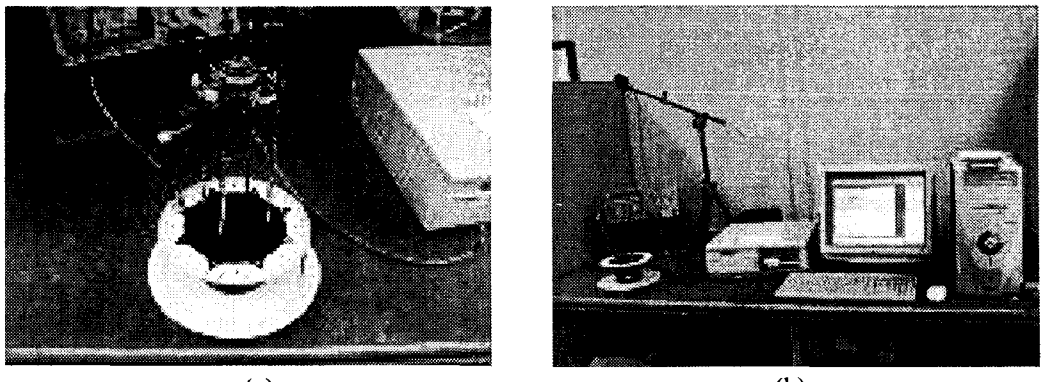

(a) (b)

Figure 7 Experimental environments with performance evaluation system. (a) Test circuit installing on the step motor apart by 60cm. (b) Whole view of test equipments, test circuit with step motor, data collection unit, PC monitor, and PC, from left side to right side.

4.2 Electrical Performances

The test results for the electrical performance of PSD are shown in Figure 8. These figures represent the output waveforms of PSD measured at the eight different directions of 45° spaces when turning the Fluxgate sensor with step angle of 2°.

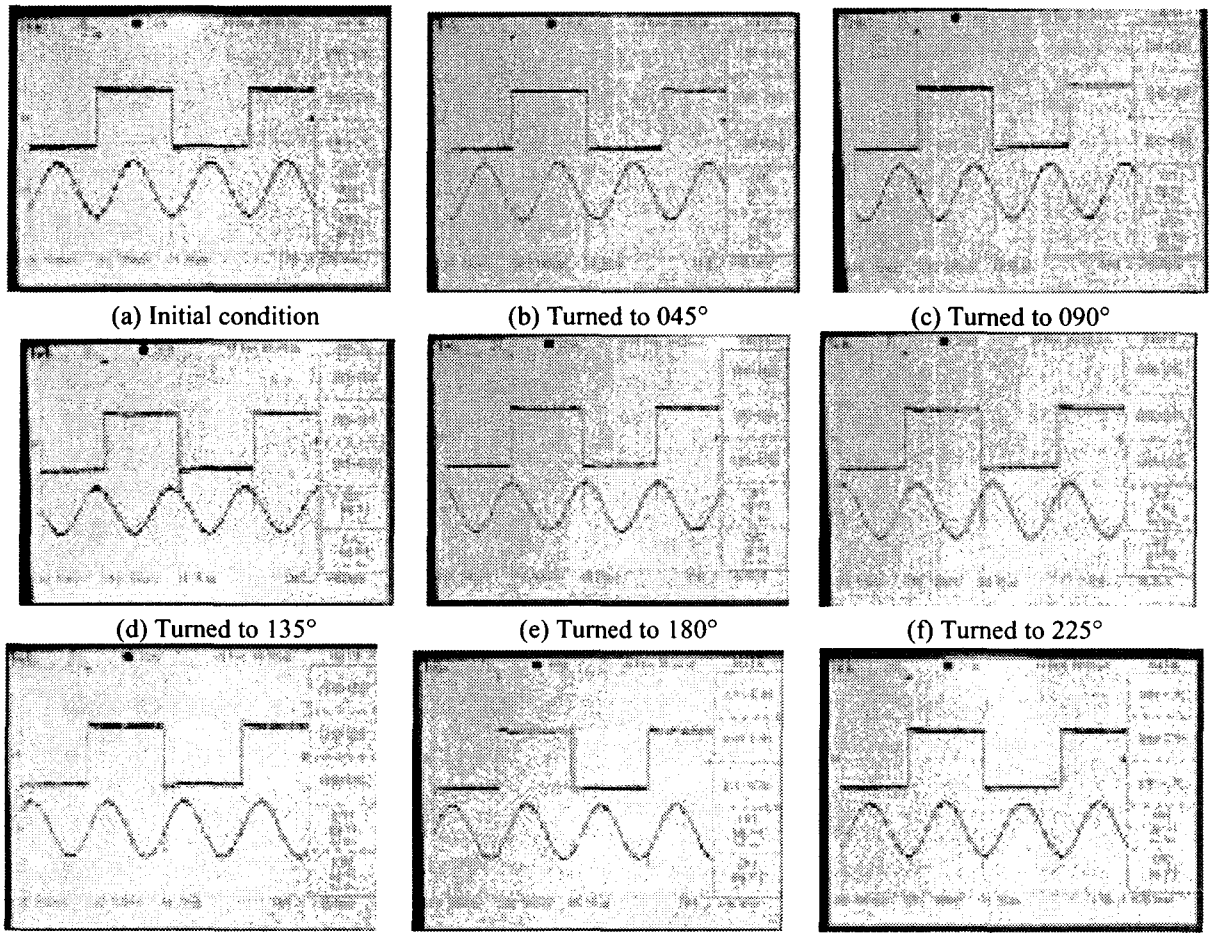

(a) Initial condition (b) Turned to 045° (c) Turned to 090°

(d) Turned to 135° (e) Turned to 180° (f) Turned to 225°

(g) Turned to 270° (h) Turned to 315° ° (i) Turned to 360°

Figure 8 Output waveforms of PSD. The upper trace and lower trace, at each figure, represent the reference signal ($2F_0$) and the output signal of PSD, respectively.

As shown in Figure 8, the phases differences between Φ_r (reference signal) and $\Delta\Phi$ (the output signal of PSD) are proportional to the given eight different directions. Thus, we know that the design of PSD circuit and Excitation circuit are successfully done in this work.

4.3 Error Analysis

The magnetic bearing data is collected with turning the test circuit with step angle of 2°. After collecting the data, error analysis is carried out with polynomial regressions. Traditionally, ship's magnetic compass adopts 8-point calibration or circular calibration to find the correction coefficients of deviation values by Fourier series. This method is to use the correction magnetic sticks by manual work. In this study, we try to find a new error analysis method except for Variations. This study is also under proceeding now.

Figure 9 shows one of the experimental results of error analysis by polynomial regressions. The bearing data of test circuit versus the reference direction are shown in Figure 9(a). The reference direction is taken from the adoption of 1st order polynomial regression to the bearing data. Thus, this connection line shows as a straight line having minimum variation of bearing data. The total difference values between the bearing data and the reference direction are shown in Figure 9(b). To draw residual errors form the total difference values, polynomial regressions with 2^{nd} order to 4^{th} order are applied as in Figure 7(c). One of the calculation results of residual errors with 4th order curve fitting is shown in Figure 7(d).

As experimental results, it is shown that the proposed method can draw residual errors influenced by host platform, and the total difference values of within ± 4° can be reduced to within ± 2°.

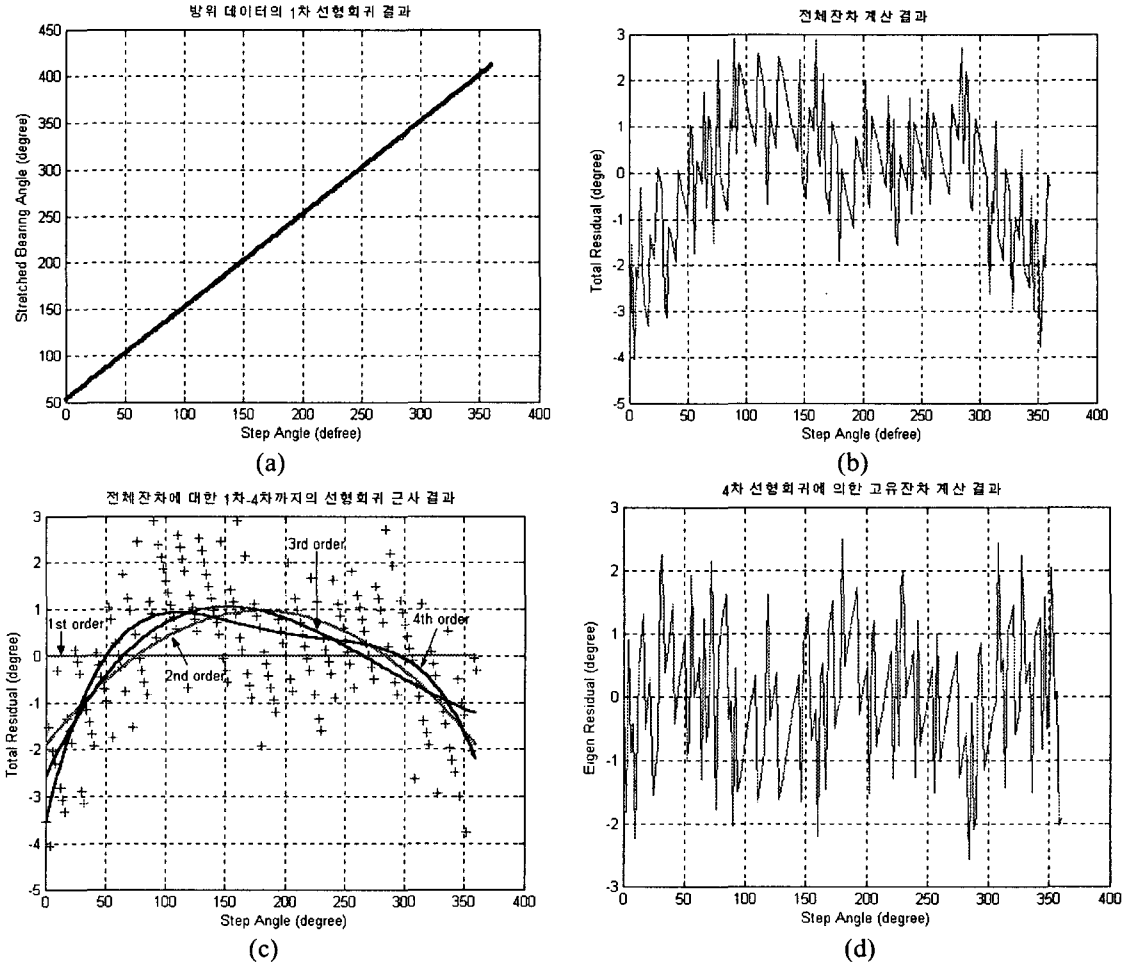

Figure 9 Error analyses by polynomial regressions. (a) Collected data and reference direction. (b) Tota difference values between collected data and reference direction. (c) Curve fitting results by polynomia regressions with 2nd order to 4th order. (d) Residuals after adopting 4th order curve fitting.

5. Conclusions

The circuit design and realization procedures are represented with discussions of some experimental results. The obtained results are summarized as:

(1) The circuit designs for the excitation part, Phase Sensitive Detector (PSD), and Digital Counter, are completed and its electrical performances are verified through tests.
(2) A new analysis method of magnetic interferences by polynomial regressions are proposed and verified.

Further, this research will proceed with two stages. In the first stage, the study will carry out to increase the resolution of Fluxgate sensor up to 0.5°. To attain this target, the study will include; establishing electro-magnetic analysis theory to find optimal design methodology of Fluxgate sensor, developing high ability performance evaluation system having vibration controller, magnetic disturbance controller, and Helmholtz coil. In the second stage, the research will go on the implementation of Digital Magnetic Compass (DMC). To attain this target, the study will include; establishing optimum design methodology to realize high resolution PSD using analog fed-back loop filter, designing FIR filter to compensate vibration with real-time, building microprocessor circuits with built-in programs to correct external magnetic disturbance. In the last, we will develop DMC with smart correction function.

Acknowledgements

This work was supported by grant No.R05-2004-000-10760-0 from Ministry of Science & Technology, Korea.

References

(1) Department of the USA Navy (1994): Technical Manual for SONOBUOYS - Basic Introduction to Air ASW Acoustic Systems, NAVAIR 28-SSQ-500-4, Direction of Commander, Naval Air Systems Command
(2) Erik B. P., Fritz P., Jan R. P. (1999): Digital Fluxgate Magnetometer for the Astrid-2 Satellite, Meas. Sci. Technol. 10, N124-129
(3) Kristin L. M. (2001): A Nonlinear Magnetic Controller for Three-Axis Stability of Nanosatellites, Master's thesis, Virginia Polytechnic Institute and State University, USA
(4) Lauro O. and Johann B. (2000): Experimental Results with the KVH C-100 Fluxgate Compass in Mobile Robots, Proc. of the IASTED International Conference Robotics and Applications 2000, Honolulu, Hawaii, USA
(5) Michael J. C., Tamara B., Carl H.S. and Robert S.: A New Perspective on Magnetic Field Sensing, Honeywell, SSEC, USA
(6) NEXEN Company in Korea: http://www.enexen.com
(7) Texas Instrument (2001), Handbook of Operational Amplifier Active RC Networks, SBOA093A
(8) United States Patent (1981): No. 4,277,751, Low-Power Magnetometer Circuit with Constant Current Drive
(9) United States Patent (1987): No. 4,677,381, Flux-Gate Sensor Electrical Drive Method and Circuit
(10) YIM J. B. (1995): Navigational Equipments, Korea Naval Academy, pp.121-124
(11) YIM J. B. (2002a): Design and Realization of Phase Sensitive Circuitry of Two-Channel Ring-Core Flux-Gate Compass, J. of KIN-PR, Vol.26 (No.1), pp.127-136
(12) YIM J. B. (2002b): Performance Evaluation System for Two-Channel Ring-Core Flux-Gate Compass, J. of KIN-PR, Vol.26 (No.5), pp.529-535